Emergent chemical behavior in mixed food and lignocellulosic green waste hydrothermal liquefaction

Heather O. LeClerc[1], Jeffrey R. Page[2], Geoffrey A. Tompsett[1], Sydney F. Niles[3], Amy M. McKenna[3,4], Julia A. Valla[2], Michael T. Timko[1], Andrew R. Teixeira[1*]

[1]Department of Chemical Engineering. Worcester Polytechnic Institute, 100 Institute Rd, Worcester, MA 01609, USA
[2]Department of Chemical and Biomolecular Engineering. University of Connecticut, 191 Auditorium Rd, Unit 3222, Storrs, CT 06269, USA
[3]National High Magnetic Field Laboratory, 1800 Paul Dirac Dr, Tallahassee, FL 32310, USA
[4]Department of Soil and Crop Sciences, Colorado State University, Fort Collins, Colorado 80523-1170, United States

*Author to whom correspondence should be addressed, arteixeira@wpi.edu

Keywords: lignocellulose, waste, food waste, synergy, mass spectrometry

Abstract

Hydrothermal liquefaction (HTL) is a promising strategy for conversion of energy-dense waste streams to fuels. Mixed-feed HTL aggregates multiple feed streams to achieve greater scales that capitalize on local resources, hence lowering costs. The potential for new pathways and products upon feedstock blending becomes a compounding level of complexity when unlocking emergent chemistries. Food and green waste streams were evaluated under HTL conditions (300 °C, 1 hr) to understand the effect of feed molecular composition on product distributions and mechanisms. Thousands of emergent chemical compounds were detected via FT-ICR MS, ultimately leading to the emergence of two dominant outcomes. First, the presence of small amounts of food waste into green waste results in substantial decarboxylation and subsequent polymerization to biocrude then chars. Second, in the other limit, small amounts of green waste promote capping of oxygenates into the biodiesel range, such as with the emergence of fatty acid methyl esters.

Introduction

To reduce the reliance on fossil fuels and counteract the effects of climate change, waste streams offer a low-carbon emission, energy-dense source to petroleum fuels. Worldwide, over 1.3 billion tons of waste are thrown away annually[1], ending up in landfills, the oceans, and scattered through the environment. Left untreated, these wastes result in fugitive greenhouse gas

emissions, cause toxic run-off, and result in algal blooms that substantially disrupt local ecosystems. By utilizing waste and diverting it from landfills, there is the potential to reduce greenhouse gas emissions by over 2.4% in the United States.[2]

Hydrothermal liquefaction (HTL) is a water-assisted thermochemical conversion process that operates at temperatures from 250 to 400 °C and sufficient pressure to maintain a liquid water phase.[3] The use of HTL has been extensively studied for the conversion of single-source waste feeds into an energy dense biocrude that is a biofuel precursor.[3-7] High-lipid feedstocks have been shown to achieve yields upwards of 40 wt.%[3, 8, 9] in comparison to the 10 – 30% yields seen with lignocellulosic HTL.[10]

HTL biocrude yields are highly dependent on feedstock compostion.[11] Lipid content plays a crucial role in HTL biocrude yields due to the inherent lyophilic nature of the constituent fatty acids.[12] The relationship between lipid content and biocrude yields means that many food wastes,[5, 13] some sewage sludges,[14, 15] and certain types of algae cultivated on wastewater[12, 16] are especially suitable for HTL. Waste biomass and low-lipid containing sewage sludge and food waste have traditionally been less desirable for use as an HTL feed primarily due to their lipid contents.[3]

Despite the prevalence of waste, it is a distributed resource that must be transported to a centralized location for processing to achieve sufficient scale to be economically viable.[17] The key parameter is waste volume per area, with greater waste generation densities permitting operation of HTL at scales that favor attractive economics without increasing transportation costs to prohibitive levels. Most economic analyses of HTL[18-20] are based on a scale of approximately 100 dry tons per day. A typical city of 100,000 people generates approximately 250 tons/day of waste, considering all types of wastes (e.g., yard waste, food waste, sewage sludge, etc.).[21] Assuming a moisture content of 50% as a reasonable value[2] implies that a mid-sized city generates sufficient waste for economical HTL, but only if multiple types of waste streams are blended together with one another. The challenge then becomes selecting the feeds to be co-fed, optimizing reaction conditions,[11, 12] and predicting the corresponding biocrude yield that can be obtained using HTL.

In addition to benefitting scale, co-feeding multiple streams to HTL can sometimes result in surprising benefits. For example, Yang et al. reported that co-liquefaction of 50% spent coffee grounds with 50% corn stalk resulted in a 20.9% increase in biocrude yield compared to either of the individual feedstocks.[22] In fact, as a rule, measured biocrude yield is rarely equal to the

expected performance predicted from physical mixing of the unique feeds and the performance of the corresponding pure streams,[23, 24] with both synergistic and antagonistic effects reported in the literature. Clearly, processes should be designed to take advantage of synergistic effects while mitigating the antagonistic effects. As shown by LeClerc et al.[25], understanding elementary reaction pathways of model compounds permits prediction of feed compositions which maximize biocrude yields. Applying a molecularly detailed pathway analysis strategy to the synergistic and antagonistic effects of co-HTL of realistic feeds is therefore a promising, yet under-developed area to maximize obtainable yields.

A recent study by Jarvis et al. advanced the understanding of co-HTL of algae and lignocellulosic feeds using Fourier transform ion-cyclotron resonance mass spectrometry (FT-ICR MS) operated in positive ion atmospheric pressure photoionization (+ APPI) mode.[23] FT-ICR MS identified at least 6,000 peaks per biocrude sample, with mixed feed biocrudes containing a higher proportion of algal-derived species than pine-derived species.[23] The work also identified > 20% unique elemental formula in biocrude obtained from algae-pine mixtures that were absent from either biocrude obtained from HTL of pure feeds.[23] Synergy was reported for processing a mixture consisting of 50% algae and 50% pine, which coincided with the increase in N_1O_3 and N_2O_3 species range identified by FT-ICR MS.[23] While the study with algae and pine points to a potential molecular interpretation of synergistic effects for mixed feeds, both algae and pine are relatively simple and comparatively expensive feeds compared with municipal wastes,[9] meaning that similar analysis is needed for abundant and inexpensive feeds like food waste and green waste.

Combined, food waste and green waste account for an estimated 1.5 billion tons per year,[2, 26] with real prices that are often negative.[27, 28] Moreover, they are co-produced in similar urban and dense suburban communities, making their mixtures an attractive feed stream for HTL. Molecularly, food and green waste are distinct from one another, and these differences are anticipated to affect their ability to be transformed into biocrude as well as the resultant biocrude composition. Food waste typically contains 40 – 60% carbon, primarily in starch, proteins, and especially lipids, and an ash content < 5%; green waste is composed primarily of cellulose, hemicellulose, and lignin, and its ash content can be greater than 10%.[25] Heteroatom content and speciation – specifically oxygen and nitrogen – are of utmost importance in determining the fate of biocrude and upgrading potential.[12, 15, 29] Here, food waste typically contains much more

nitrogen than green waste, with most of the nitrogen content in organic forms associated with proteins.[25] Oxygen in the dominant heteroatom present in green waste, arising from the glycosidic linkages and hydroxy and acetyl sidechains of cellulose and hemicellulose.[12, 30] The presence of multiple, poorly defined types of chemicals in food waste and green waste opens a wide range of potential pathways for biocrude formation that must be understood for selection of optimized blending ratios in HTL feed streams.

In this work, a cafeteria food waste and a lignocellulosic green waste were mixed in five blending ratios and used as HTL feeds. Yields of biocrude as well as the char, aqueous phase, and gas byproducts were measured, with the objective of identifying synergistic and antagonistic phenomena, with synergism and antagonism defined based on the performance of the pure feeds. The resulting biocrudes were then analyzed using gas chromatography and FT-ICR MS to identify molecular-level differences that give rise to synergism and antagonism.[23] The results of this study advanced current understanding of the molecular-level phenomena that arise from co-HTL of real-world waste streams, a key step toward technological implementation.

Materials & Methods

Materials.

Food waste was obtained from a veteran's hospital cafeteria (via Greener Chemistry LLC.). An Ecovim dehydrator was used to pre-grind and dry the food waste, which was then stored in a freezer at −20 °C prior to use. Green waste, consisting of grass, wood chips, and yard clippings, was obtained from BDP Industries Inc., Greenwich, NY. Green waste was placed in air-tight bags and stored in a freezer at −20 °C. Green waste was removed from the freezer, dried, ground, and sieved to < 0.85 mm particle size immediately before use. Both food waste and green waste were dried in an oven at 60 °C overnight prior to weighing so that the slurry fed to reactor could be fixed at a solids loading of 15 wt.% dry weight.

Other reagents included >99.5% pure acetone (Sigma Aldrich), which was utilized for biocrude recovery and cleaning; deionized water with electrical resistivity greater than 18.0 MΩ, which was used to prepare feedstock slurries; and gases. Nitrogen gas (purity >99.9%, Airgas) was used to purge air from the reactor and to pre-pressurize it to ensure a liquid water phase was present during HTL. Helium (grade 5.0, Airgas) was used as the carrier gas for GC analysis.

Table 1. Food and green waste feedstock properties from proximate, elemental, and biochemical analysis.

	Food Waste	Green Waste
Proximate Analysis (wt.%) [a]		
Moisture [b,e]	0.7 ± 0.1	0.5 ± 0.2
Ash [f]	1.9 ± 0.9	14.1 ± 1.3
Elemental Analysis (wt.%) [a,e]		
Carbon	52.2 ± 0.9	42.2 ± 0.1
Hydrogen	7.5 ± 0.2	5.2 ± 0.2
Nitrogen	4.3 ± 0.1	0.2 ± 0.1
Sulfur	1.0 ± 0.1	0.7 ± 0.2
Oxygen [c]	33.2 ± 2.1	51.7 ± 1.8
Biochemical Analysis (wt.%) [a,e]		
Carbohydrates	29.8	-
Holocellulose	-	69.7
Lignin	-	16.2
Lipids	38.9	-
Protein [d]	26.8 ± 0.6	-
H/C_{eff}	0.55	-0.39
HHV(MJ/kg)	23.6 ± 3.0	13.5 ± 0.6

[a] Dry basis. [b] As received. [c] Oxygen determined by difference. [d] protein = N content * 6.25. [e] standard deviation reported as ± where n = 3, [f] Standard deviation reported as ± where n = 2.

Hydrothermal Liquefaction Reactions.

HTL reactions were conducted in a 300 mL Parr stainless steel batch reactor, as has been previously described.[31, 32]. Reactions were completed at 300 °C and approximately 200 bar to ensure water remained in the liquid phase. Heat-up required approximately 45 min. After a pre-determined 60 min reaction time, the reactor was quenched in an ice bath to < 40 °C. Quenching required approximately 10 min.

After quenching, biocrude and solids were separated from the aqueous phase via vacuum filtration after which the biocrude and solid phases were separated from one another using acetone. Acetone was stripped from the biocrude using rotary evaporation set at 40 °C and 350 mmHg to maximize solvent removal and minimize biocrude losses. Representative samples of the stripped acetone were analyzed and found to have purities >99% and indicative of <1% biocrude loss during evaporation. The mass of the gas phase was determined by difference between the reactor mass before and after venting. The masses of the gas, aqueous phase, solid, and biocrude products were

summed and compared with the mass charged to the reactor to close the overall mass balance. In all cases, data reported here correspond to overall mass balance closure > 90%. Losses represent residual material that could not be removed from the reactor, transfer losses, and the precision of the analytical balance used to estimate gas yields (± 0.5 g).

Product Analysis. Products were analyzed gravimetrically, by elemental composition, and by molecular composition using a combination of methods that have been described previously in the literature for similar applications. Analytical methods are described briefly here, with further details on characterization techniques found in previous papers[25, 32, 33] and the Supporting Information.

Elemental analysis (CHN) was utilized to determine the carbon content of the biocrude and char phases (Midwest Microlabs, Indianapolis, IN). Total organic carbon (TOC) measured the carbon in the aqueous phase, and gas-phase carbon was assumed to be 98% CO_2 based on previous studies.[31, 32] The feedstocks and biocrudes were also sent to Mainstream Engineering (Rockledge, FL) for higher heating value (HHV) analysis using a Parr Instruments semimicro calorimeter. Energy recovery was calculated based on the gravimetric biocrude yield and its measured HHV. Masses of the gas, aqueous phase, char, and biocrude products was converted into carbon terms using the aforementioned elemental analysis methods and compared with the initial carbon charge. In all cases, the carbon balance closed to within 5%.

Gas chromatography mass spectrometry (GC-MS) (Agilent 6890N equipped with a 5973N mass spectrometer) was performed on all biocrude samples to determine chemical composition of products with normal boiling points < 300 °C. Further GC-MS method details have been reported previously.[25, 31] Individual compounds were identified based on similarity with a built-in mass spectral database;[34] only compounds with matches >80% are reported here.

Fourier-transform attenuated total reflectance infrared spectroscopy (FT-ATR-IR) was used to analyze the functional group content of biocrude and char products. A Shimadzu FT-IR spectrometer equipped with a QATR-S single reflection ATR cell and with a resolution of 8 cm^{-1} was used for all measurement. Spectra were compared with known databases[35, 36] to identify bands attributable to specific functional groups.

Biocrude samples were further analyzed using positive-ion atmospheric pressure photoionization 21 Tesla Fourier-transform ion cyclotron resonance mass spectrometry (+APPI FT-ICR MS).[37, 38] Samples were dissolved in a 50/50 (by volume) mixture of toluene and tetrahydrofuran to a final concentration of 125 µg/mL prior to analysis. Further details on FT-ICR MS methodology can be found in the Supporting Information.

Thermal gravimetric analysis (TGA) was performed on a Shimadzu TGA-50. The heating rate was set to 10 °C/min and samples were heated from 25 to 800 °C under a constant nitrogen flow rate of 25 mL/min.

Results

This work aims to identify and understand the chemical interactions between lignocellulosic and food-based components that occur during co-HTL. To produce a series of feeds with intermediate compositions, five feedstocks were studied: one consisting of a food waste sourced from a veteran's hospital cafeteria, one green waste sourced from a local composter, and three blends corresponding to ratios of 75 wt% food waste (75:25), 50 wt% food waste (50:50), and 25 wt% food waste (25:75). These five feeds were treated under HTL conditions (300 °C and 1 hr. reaction time) selected to be representative of conditions commonly used for HTL.[25, 31, 32] The product mixture was quantified for yields of solvent-soluble biocrude, water-soluble aqueous phase, solid char, and gaseous products. The biocrude was further analyzed using GC-MS, FT-IR, TGA, and FT-ICR MS to capture the molecular composition and as the basis for understanding the chemical interactions.

HTL Feed Characterization.

Feedstock compositions provided in **Table 1** show that food waste has greater carbon and hydrogen content and higher heating value (HHV) than green waste; differences are attributable to lipid content in the food waste and the combined cellulose and hemicellulose content of the green waste. Similarly, the effective hydrogen to carbon ratio (H/C_{eff}) of food waste is greater than that measured for green waste (**Table 1**). H/C_{eff} is calculated as: $\frac{H}{C_{eff}} = \left(\frac{H-2O-3N-2S}{C}\right)$, and is a measure to describe the potential of a feed to be economically converted into biocrude with a final $H/C_{eff} > 2$.[39, 40] **Figure 1** shows that biocrude yields increase with increasing $H/C_{eff,}$ as H/C_{eff} increases with increasing food waste content. Accordingly, the H/C_{eff} values reported in **Table 1**

indicate that HTL conversion of food waste should be expected to lead to the greatest biocrude yield and energy recovery (**Figure SI-1**) and green waste the least, with HTL conversion of mixtures producing intermediate biocrude yields weighted by their blending ratios. **Table SI-1** provides further characterization data on the two feeds.

HTL Product Yields.

HTL conversion of organic wastes produces biocrude, char, aqueous, and gas products. Gravimetrically determined carbon yields of these four products are shown in **Figure 1**. Dashed lines represent the linear weighted average between the two pure feeds (HFW and GW) corresponding to the expected physical mixture of food and green waste in the absence of any synergistic or emergent effects. Data in **Figure 1** show that increased food waste content results in increased biocrude yield (carbon wt.%), consistent with the carbon and lipid content of food waste and the H/C_{eff} analysis discussed earlier.

Figure 1 reveals the presence of emergent behavior for several feeds. A synergistic effect on the biocrude yield is observed for the 75:25 food waste:green waste mixture, corresponding to a biocrude yield increase of 14.4% relative to the expected weighted average performance. On the other hand, an antagonistic effect is observed for the 25:75 food waste:green waste mixture, which produced 13.8% less biocrude than expected based on the yields observed for the two pure feeds. The effects on biocrude yield are mirrored by decreases in char yields for the 75:25 mixture and corresponding char yields increases for the 25:75 mixture. Taken collectively, the biocrude and char yield data shown in **Figure 1** indicate that synergistic effects between food waste and green waste reactants can shift carbon away from char-producing pathways and into biocrude-producing ones; antagonistic interactions have the opposite effects.

A final trend can be observed in **Figure 1** regarding the gas formation. All blends resulted in increased gas levels compared with the individual wastes, with carbon dioxide present as the dominant gas-phase product. Gaseous products are resultant of the deoxygenation and especially decarboxylation reactions, suggesting that emergent chemical pathways are able to promote these pathways. Gas yields observed for the 25:75 food waste:green waste blend, which was 58% greater than predicted based on behavior of the pure feeds, are especially noteworthy. The gas yields observed for mixtures are further corroborated by elemental analysis, which shows blended

feedstocks result in biocrudes with decreased oxygen content compared to the levels expected from the pure streams (**Table SI-3**).

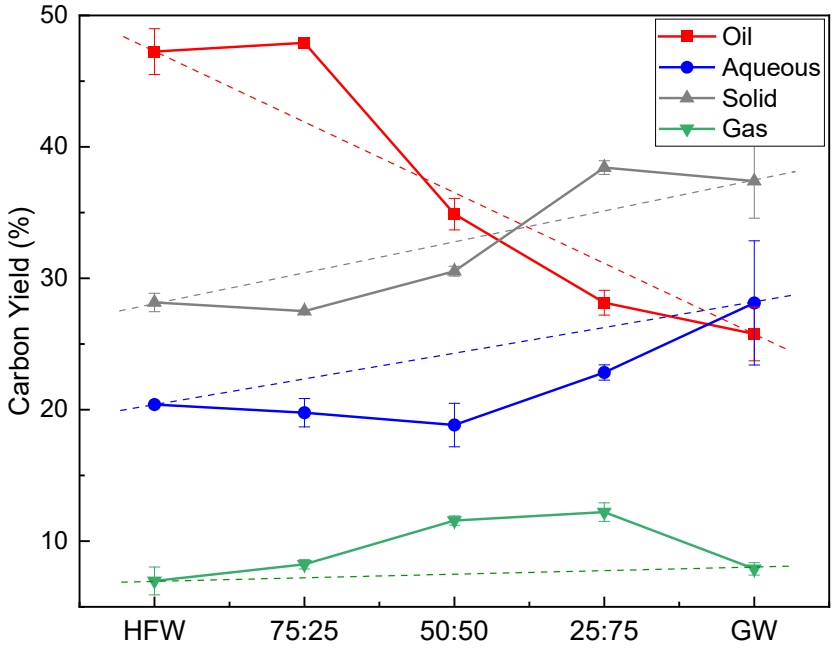

Figure 1. Hydrothermal liquefaction product yields, expressed as carbon yield, for mixtures of food and green waste. Dashed lines represent the expected, theoretical trend if performance were a linear combination of pure food waste and pure green waste. Error bars represent the standard deviation from performing at least two runs.

To understand the emergent behavior indicated by carbon yields in more detail, biocrude samples were analyzed using thermogravimetric analysis (TGA). **Figure 2** shows the results, quantified into fractions based on volatility corresponding to gasoline (< 190 °C), jet fuel (190 – 290 °C), diesel (290 – 340 °C), vacuum gas oil (340 – 540 °C), and residue (> 540 °C). TGA indicates that gasoline is the most abundant of these fractions in the green waste-derived biocrude, consistent with the decomposition of cellulose and lignin into C_6-C_{12} oxygenates. In contrast, jet fuel is most abundant component in the food waste biocrudes, consistent with C_{12}-C_{18} fatty acid content. Further analysis reveals that blending causes a decrease in the percentage of compounds in the residue range in mixtures of 75:25, containing only 0.5% of compounds, compared to the predicted 10%. Instead, blending at this ratio caused a corresponding increase in diesel range molecules. On the other hand, 25:75 food waste-green waste mixtures caused a sharp increase in gasoline-range molecules, nearly 10% above the expected value of 21%, as can be seen in **Figure SI-2**.

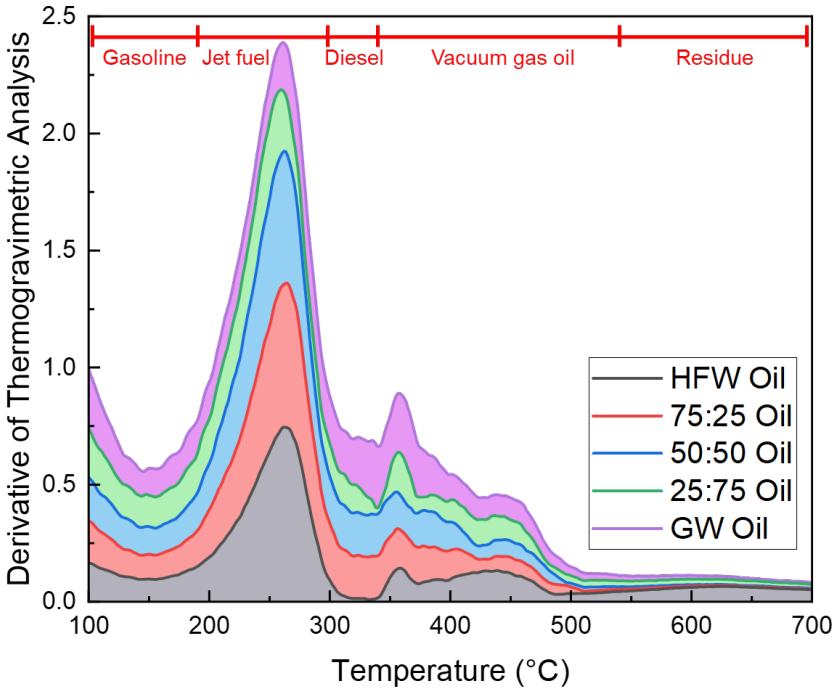

Figure 2. Stacked thermogravimetric analysis (TGA) differential mass loss percent plotted as a function of temperature. Temperature ranges were chosen to match those reported in Haider et al.[41] Gasoline = <190 °C, jet fuel = 190-290 °C, diesel = 290-340 °C, vacuum gas oil = 340-540 °C, residue = >540 °C. Compounds associated with mass loss at T > 540 °C can also be termed asphaltenes.

TGA further indicates that less than 60% of biocrude compounds are analyzable with gas chromatography (T< 325 °C), with food waste biocrude yielding a higher analyzable fraction than green waste. Green waste biocrude, however, has a high concentration of residue-range compounds with vaporization temperatures above 500 °C, leading to only 37% of its mass loss occurring at temperatures less than 300 °C. The remaining samples' percentage of GC-amenable compounds are summarized in **Table SI-4**.

Biocrude Molecular Characterization.

TGA shows that approximately 60% of the food waste biocrude is amenable to GC analysis whereas only 37% is in green waste biocrude. To analyze the non-volatile biocrude fraction, 21 tesla (+) APPI FT-ICR MS was used to obtain high resolution (50 ppb) mass spectra of ionizable components heavier than approximately 100 Da. Ionization efficiency is determined by the molecular structure of the analyte mixture, and the polydispersity and polyfunctionality of biofuels

result in a range of species with different ionization potentials, and APPI is more selective towards aromatic species found in green waste.

FT-ICR-MS of each of the five samples, revealing the presence of thousands of compounds in each of them, are shown in **Figure 3**. Molecular species from each mass spectrum range from 9,000-15,000 elemental compositions, with a total of ~60,000 species identified across all samples. **Figure 3** shows that only 4,199 species were identified as common across all samples, highlighting the abundance of unique species identified with different feedstock combinations. Specifically, 165 (1.8%) and 2,470 (19.9%) species are unique to food waste and green waste biocrude, respectively, whereas green waste and 25:75 biocrude accounted for over 4,000 unique elemental composition assignments—almost 10% of the total number of species identified.

Molecular identification by FT-ICR MS highlights hundreds of unique compounds from each biocrude and indicates unique chemical interactions between food and green waste components. Food waste biocrude contains only 165 unique species, 15-times fewer than green waste biocrude, which is likely due to differences in aliphatic and aromatic content of these two feeds (see Table 1). In particular, green waste lignocellulosic content reacts to form highly aromatic oxygenated compounds that are more efficiently ionized by atmospheric pressure photoionization than more aliphatic (e.g., fatty acids and carboxylic acids) compounds found in food waste. Food waste consists of a significant aliphatic component from fatty acids; aliphatic compounds are less efficiently ionized by atmospheric pressure photoionization, hence the relatively small number of unique species identified in the food waste biocrude may be attributable to the importance of aliphatic molecules in this sample.

Taking this analysis a step further, the black outline encompassing the hash-marked region in **Figure 3** denotes the area of elemental compositions found in the pure feedstock and represents physicochemical interactions retained upon mixing. Outside this shaded region are emergent species, which arise from reactive chemistry to produce species not found in either pure feed (8.0% of identified elemental compositions). Venn diagram analysis helps to identify the presence of emergence, it does not: a) provide information on the chemical makeup or heteroatom distribution of the emergent species, or b) quantify differences in non-emergent species to identify pathways enhanced or suppressed by blending food and green waste biomolecules in varying ratios at HTL conditions. Since (+) APPI FT-ICR MS provides elemental composition assignments, qualitative,

compositional trends between the samples can be visualized based on heteroatom class and degree of aromaticity.

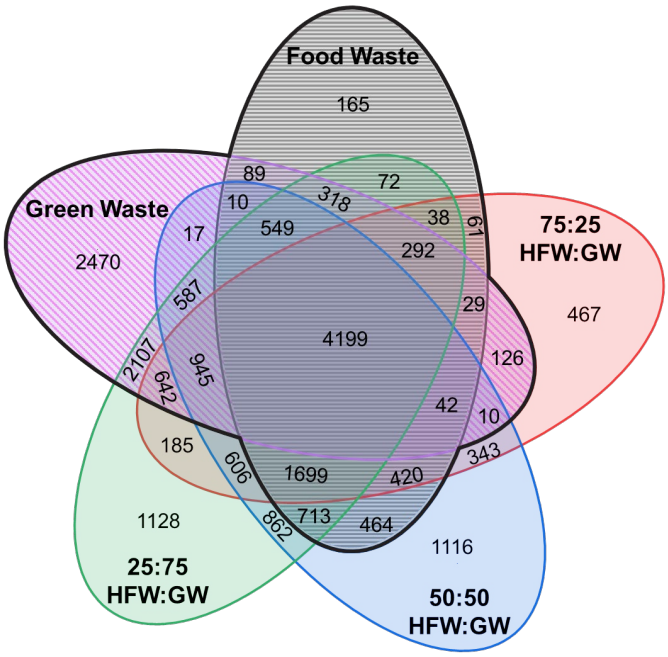

Figure 3. Venn diagram depicting the number of elemental compositions derived from (+) APPI FT-ICR MS at 21 tesla shared between the five biocrude samples. The total number of molecular species identified in each sample: HFW: 9,160; 75:25: 10,104; 50:50: 12,582; 25:75: 14,942; GW: 12,432. The outer envelope (not hashed) is the number of unique species not found in any of the other biocrudes.

To understand the compositional differences in greater molecular detail, the biocrude products were analyzed using FT-IR to identify functional groups and GC-MS to identify specific molecules present in the biocrude volatile fraction. **Figure 4a** provides FT-IR spectra showing the fingerprint regions of the five biocrude samples comprising this study. In all cases, a band attributable to the carbonyl stretch and a second band attributable to the C-O stretch are present in the spectra. The position of this band does not change between spectra, occurring at ~1700 cm^{-1} in all cases, representative of a carboxylic acid or conjugated acid. The strong C=O stretching band in HFW biocrude is consistent with carboxylic acids from food waste's high lipid content, whereas the same band in GW biocrude is more likely attributable to conjugated sugars.

In addition to these common features, the individual biocrude spectra contain substantive variations from one another. The spectra of green waste and 25:75 HFW:GW biocrudes contain

strong evidence of phenolic groups (**Table SI-5**), as indicated by bands at 1516, 1330, 1200, 1114, 1092, and 1030 cm^{-1}.[36] The family of phenolic bands decrease in intensity as the percentage of food waste in the feed increases, disappearing entirely in the spectrum of pure food waste biocrude, indicating the absence of phenolic compounds in food waste biocrude. Similarly, a band located at 1469 cm^{-1} and attributable to the CH_2 stretching mode of alkanes increases in intensity with increasing food waste content, a finding which is consistent with hydrolysis of lipids to produce fatty acids.[35]

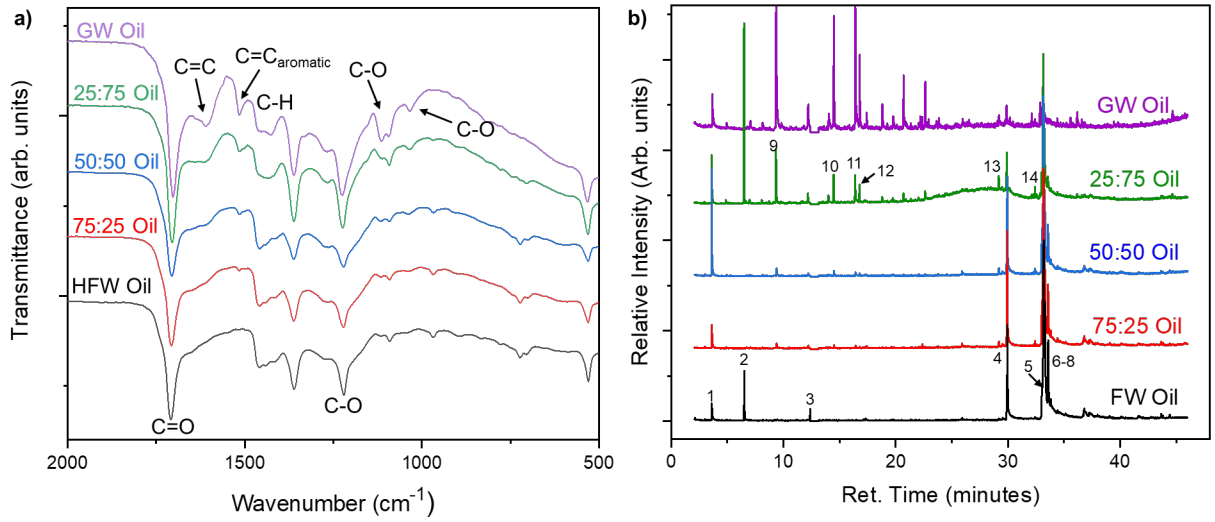

Figure 4. a) Fourier-transform infrared spectroscopy (FT-IR) spectra of the five biocrudes obtained from mixed-feed HTL. **b)** Gas chromatography (GC-MS) spectra of the five biocrudes. Peaks with identification confidence score greater than 80% are numbered. Number identities can be found in the Supporting Information (Table SI-5).

FT-IR provides some general information about functional groups present in the biocrude, but on its own cannot explain the observed emergent behavior in the FT-ICR MS and arising from synergistic or antagonistic interactions between food waste and green waste compounds. Next, samples were analyzed using GC-MS for the characterization of the light biocrude compounds, defined here on a volatility basis as compounds with a normal boiling point less than 300 °C. Spectra are shown in **Figure 4b** with peaks corresponding to >80% matches on the mass spectra data base search numbered (see the Methods Section for more details). GC-MS spectra of food waste contain C_{16} and C_{18} fatty acids (peak numbers 4-8) as the most prominent peaks, with the intensities of the corresponding peaks decreasing in intensity with increasing green waste content in the feed. The fatty acid content of the food waste biocrude identified is consistent with the FT-

IR spectra shown in **Figure 4a** and is the expected outcome of lipid hydrolysis to form biocrude-soluble fatty acids.[12] The chromatogram obtained from the green waste biocrude is dominated by highly volatile, low retention time phenolic derivatives such as methoxyphenol (peak number 9) and ethylguaiacol (peak number 10). These peaks are also present in the 25:75 food waste: green waste chromatogram and are the putative breakdown products of lignin present in green waste. The identification of individual phenolic products in the biocrudes derived in whole or in part from green waste is entirely consistent with the FT-IR spectra shown in **Figure 4a**, providing a mutually consistent interpretation.

Whereas fatty acid and phenolic biocrude components can be explained entirely by physical mixing effects, several other peaks shed light on emergent behavior that can only be explained by chemical interactions. Specifically, peaks 13 and 14 in **Figure 4b** can be attributed to hexadecenoic acid methyl ester and octadecanoic acid methyl ester, respectively. Octadecanoic acid methyl ester is one of a class of compounds called fatty acid methyl esters (FAMEs)[12, 13] that appear in the greatest concentration in the 25:75 biocrude and are present in the 50:50 and 75:25 biocrudes in small quantities but absent from the food waste biocrude. The presence of FAMEs cannot be explained entirely by physical mixing of the two parent biocrudes and must instead be explained by chemical interactions. In this case, the probable explanation is reaction between methanol, formed as a hydrolysis product of methoxy phenols,[42] and fatty acids. The high temperatures and acids present in the HTL reaction mixture facilitate their reaction.[42]

Compositional comparison: Heteroatom class distribution by APPI FT-ICR MS at 21 T.

Figure 4 helps explain the compounds that commonly occur in the various biocrudes, their physical mixtures, and some of the emergent behavior anticipated from **Figure 3**. That stated, the signs of emergent behavior apparent in **Figure 4** are admittedly subtle and cannot, on their own, explain the phenomena observed in **Figure 3**. The implication is that the emergent products must possess similar functional groups as those present in the pure feeds and further that the emergent products are present primarily in fractions of the biocrude that are insufficiently volatile for GC analysis. Accordingly, the FT-MS data were re-analyzed to mine further molecular-level details for evidence of emergent behavior.

Figure 5 shows the heteroatom class distribution derived from 21 T +APPI FT-ICR mass spectra of each biocrude. The most abundant class in the green waste biocrude corresponds to

species with six oxygen (O_6), which is typical of cellulosic feedstocks made up of a glucosidic backbone. While this fraction naturally decreases in blends of decreasing fractional green waste in the feed, the decrease is greater than anticipated based simply on mass balance considerations. The dashed lines in **Figure 5** represent the weighted average of relative abundances in each class for individual feed distributions. These dashed lines can be considered to be the expected distributions of a physical blend with no emergent behavior. Any deviation from this line represents emergent behavior that either promotes or suppresses the formation of each group upon blending of the feedstocks. The largest variance occurs in classes with five or more oxygen, which are diminished upon blending with GW. Interestingly, while all blends have decreased oxygenate heteroatom abundance relative to the value expected from physical mixing, the reduction is most exaggerated in the 50:50 and 25:75 blends, where the most deoxygenation was observed in **Figure 1** and attributed to emergent or synergistic formation of CO_2. This is further supported by the data shown in **Figure SI-3** which contains the H, N, and O content of the biocrudes, showing a 30% oxygen reduction in the 50:50 biocrude compared to the expected value.

Figure 5b shows data obtained from elemental analysis corresponding to nitrogen reduction relative to the feed. Increasing GW fraction results in increases in the relative abundance of nitrogen-containing species to values greater than predicted by simple additive mixing, suggesting that emergent behavior partitions more nitrogen into the biocrude diverting from the char or aqueous phases. This is also consistent with the proximate analysis which observed elevated nitrogen in the blends (**Table SI-3**). Collectively, these comparisons indicate that the decrease in oxygen class abundance is not a bulk change in the partitioning of oxygen, but instead due to interactions between intermediates to create new nitrogen-oxygen compounds. The differences in abundance from the theoretical prediction in the N_xO_y classes and O_y classes in the 50:50 biocrude results in similar HHV for the 50:50 and 75:25 biocrudes at 34.2 MJ/kg, and 34.3 MJ/kg, respectively.

Species that contain six oxygens (O_6) correspond to the average relative abundance in the green waste biocrude. Molecules that contain six oxygen are consistent with cellulose and potentially lignin precursors. Of these, the glucose backbone of cellulose has the molecular formula $C_6H_{12}O_6$, which would apparently give rise to O_6 heteroatom products. On the other hand, lignin is composed of an array of cross-linked phenol-derivatives as well as furans, each containing

one oxygen. Incomplete depolymerization of lignin has the potential to produce large ionizable molecules with six oxygens.[43, 44] However, the molecular weight of glucose (180.16 g mol^{-1}) is on the cusp of potentially identifiable compounds by FT-ICR MS and the low K_{OW} (0.001) of glucose indicates that it would not partition to the biocrude upon separation. Lignin oligomers with six oxygen atoms would be much larger than glucose, owing to differences in oxygen content in lignin and cellulose, and lignin oligomers would have greater biocrude solubility than simple sugars. These considerations strongly suggest lignin as the primary source of these observed O_6 compounds present in GW-derived biocrudes.

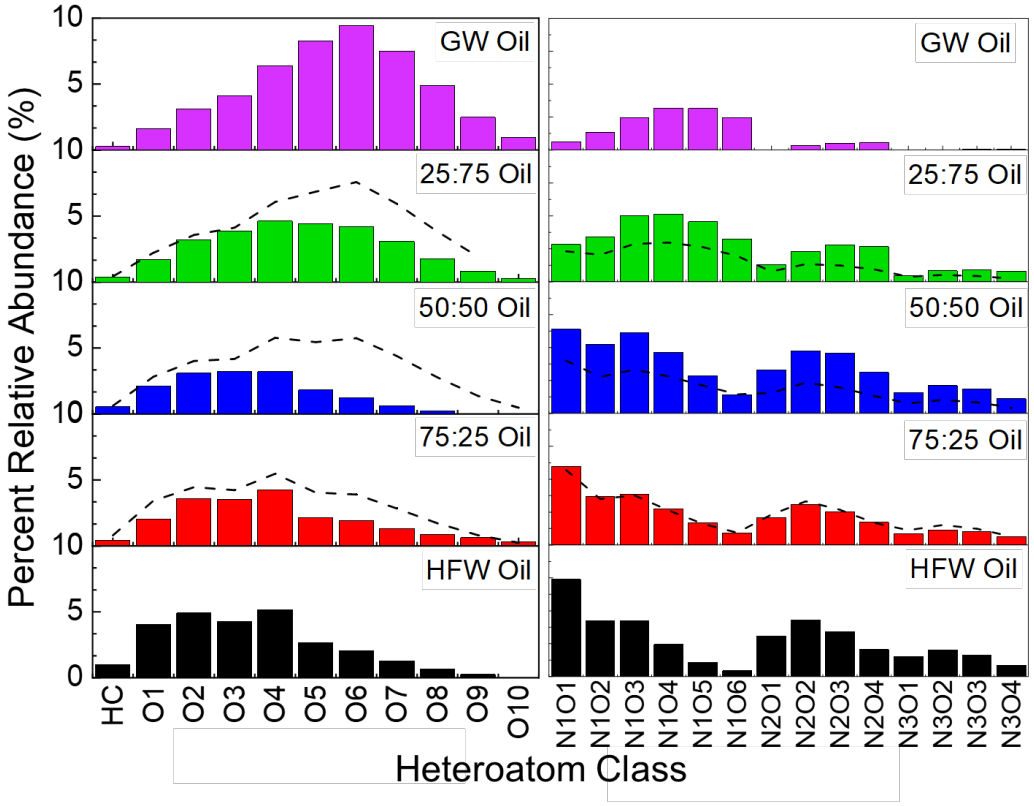

Figure 5. a) Oxygen heteroatom class distributions derived from 21 tesla (+) APPI FT-ICR MS mass spectra of the five biocrudes. **b)** Nitrogen-oxygen heteroatom class distributions of the five biocrude samples. The dashed lines are a model depicting the predicted weighted average of food and green waste component contributions.

Compositional Trends: DBE versus carbon number

Because FT-ICR MS provides elemental composition assignment, compositional trends within heteroatom classes can be rapidly visualized by plotting double bond equivalents (DBE,

number of rings plus double bonds to carbon, calculated from the elemental composition DBE = $C - H/2 + N/2 + 1)$[45] for each class. **Figure 6** plots DBE versus carbon number for only the unique species identified in each biocrude for a suite of nitrogen-oxygen heteroatom classes.

The differences in compositional space coverage seen in **Figure 6** provide details on the effects of feedstock mixing. All shades of gray represent species identified in at least two of the mixed-feed biocrudes whereas red, blue, and green represent those species unique to 75:25, 50:50, and 25:75 biocrudes, respectively. Light blue species are those identified in all five biocrude samples. From this analysis, it can be seen that the majority of the emergent species in the $N_1O_{1\text{-}4}$ classes occur at larger carbon numbers (between 30 – 40) than they appear in food and green waste biocrudes. Unique species in the N_1O_1 class span the full range of double bond equivalents from one to twenty, an indication that emergence is not specific to green waste-derived aromatic compounds nor to aliphatic food waste compounds, but instead represent the condensation of the two species types.

The FT-ICR MS data presented here begins to provide further details on the chemical makeup of the observed emergent behavior. The DBE vs. carbon number plots in **Figure 6** provide information on the differing distributions for select heteroatom classes produced by each biocrude and the apparent increase in carbon number range with the addition of green waste. The increased carbon number can be seen clearly in the N_1O_3 and N_1O_4 classes, wherein the region with carbon number greater than 30 and DBE greater than 20 are nearly solely populated by green waste biocrude species—these species no longer appear in the presence of food waste, suggesting that they are a reactive fraction that likely lead to formation of the heavy emergent species observed in N_2O_3 and N_2O_4 classes. Similarly, the N_2O_4 class highlights the emergence of species in this same region in the 25:75 biocrude. With carbon number greater than 35 and the knowledge of the heteroatom class, this can be attributed to polymerization reactions between protein-derivatives and sugar-derivatives, i.e., the Maillard reaction.

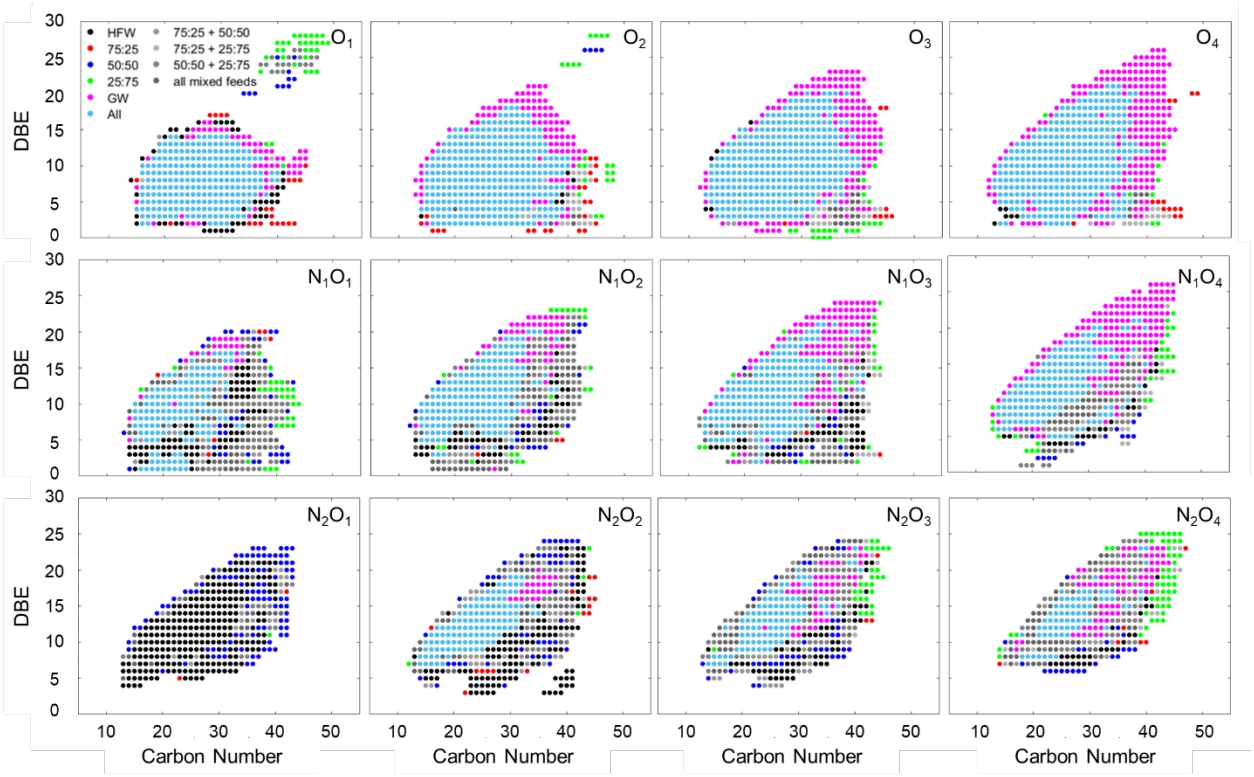

Figure 6. Double bond equivalency as a function of carbon number for the $O_{1\text{-}4}$, $N_1O_{1\text{-}4}$, and $N_2O_{1\text{-}4}$ heteroatom classes depicting species derived from the (+) APPI FT-ICR mass spectra of the five biocrude samples. Species present in food waste biocrude in black and green waste biocrude are shown in magenta. Shades of gray are indicative of species unique to more than one of the mixed feeds, whereas red, blue, and green indicate species unique to the 75:25, 50:50, and 25:75 biocrude, respectively. Light blue species are those shared by all five biocrudes.

The most reactive components present in food waste can be determined by identifying which unique species disappear upon blending. In **Figure 6,** the N_2O_1 heteroatom class visually stands out from the rest due to the lack of light blue and magenta, and the dominance of black points that represent the fraction of green waste that otherwise reacted in blends. Those reactive points (black) generally represent the low-oxygen containing light compounds. These are likely protein derivatives, such as amino acids and short chain peptides that would otherwise readily react with oxygenates to form the larger emergent molecules upon feedstock blending with green waste. Furthermore, the prevalence of emergent compounds in the 50:50 biocrude (blue) is observed within the N_2O_1 class, primarily occurring at carbon numbers above 35 and DBE greater than 15. These species are most likely the result of the interaction between green waste-derived oxygenated aromatics with protein-derivatives in Maillard-type reactions, which were previously shown to be dominant at stoichiometric ratios of proteins (food waste) and oxygenates (green waste).[25] This

finding supports the previous hypothesis for FAME production, wherein highly aromatic molecules derived from lignin and cellulose react with straight chain molecules from lipids and less aromatic molecules in protein[25] to increase the relative abundance of compounds with intermediate DBE values.

Figure 7 represents modified van Krevelen plots of emergent species used to elucidate the effect of nitrogen and oxygen heteroatoms on the biocrude formation. **Figure 7** shows an interesting molecular weight periodicity that appears in the 50:50 biocrude as N/C and O/C ratio increase. Increasing heteroatom content, i.e. N_2, N_3, results in a dampening effect wherein H/C ratio spans the entire range in the N_1 range and decreases to 1 – 2. The dampened periodicity with heteroatom content corresponds to the addition of one nitrogen or one oxygen, a potential clue into polymerization reactions. The periodicity in O/C ratio is seen clearly in the emergent molecules (**Figure SI-5**), formed by the interaction between nitrogen-containing protein in the food waste with heavy oxygen-containing lignin molecules. The overall shape of the data is indicative of increased aromaticity in high N/C and O/C ratio compounds, as the maximum H/C value in **Figure 7a and b** decreases from nearly 2.5 to 1.5.

Figure SI-4 shows the modified van Krevelen diagrams colored by molecular mass for the biocrudes obtained from food and green waste feedstocks, highlighting that the recurrent trend in molecular weight seen in **Figure 7** is emergent and not present as clearly in biocrudes obtained from either of the pure feeds. The areas of high molecular weight (MW > 600) repeat every 0.025 in N/C, corresponding to the approximate addition of 1 nitrogen for 36 carbon. These periodic repeating distributions are consistent with the expectation that reaction intermediates have molecular distributions similar to their constitutive amino acids; for each monomer containing one nitrogen (N_1), for example, there is a distribution of carbon numbers (glycine N/C = 1/2; phenylalanine N/C = 1/9). Furthermore, for each monomer, there is also a distribution of number of nitrogen atoms (glycine N = 1, arginine N = 4). These two distributions within the feed material result in overlapping yet periodic distributions. The same trend holds true with oxygen-containing intermediates. It is also important to remember that only emergent molecules are shown, indicating that this pattern is based on the interaction between food and green waste components.

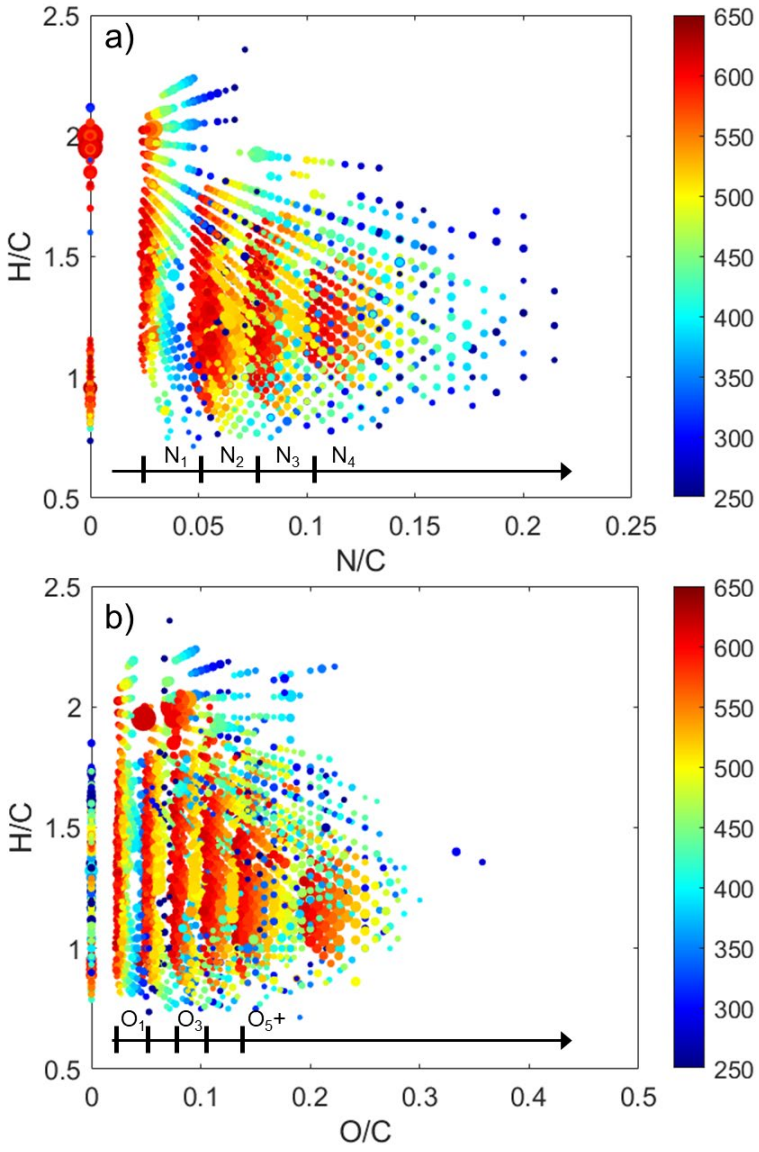

Figure 7. (a) Modified van Krevelen plot comparing H/C ratio to N/C ratio for the emergent molecules identified in the 50:50 biocrude colored by molecular mass (determined by m/z ratio). (b) Van Krevelen plot comparing H/C ratio to O/C ratio for the emergent molecules identified in the 50:50 biocrude colored by molecular mass.

Repeating units in O/C ratio (**Figure 7b**) are similar in magnitude to those for nitrogen (**Figure 7a**), occurring with a period of 0.023 O/C. More interestingly, however, is that biocrudes from pure food and green waste do not exhibit the same strong trend in O/C ratio (**Figure SI-4**). At O/C < 0.1, food waste biocrude begins to show the same periodicity but the trend disappears above this ratio, whereas green waste biocrude has a region of high molecular weight compounds spanning from 0.1 – 0.3 O/C and centered around H/C of unity. The presence of emergent

molecules in **Figure 7b**, however, are clearly visible across all O/C ratios, further corresponding to an increase in oxygen number as supported by **Figure SI-4**. The appearance of this trend upon mixing food and green waste supports interpretation of a synergistic polymerization wherein oxygen-containing molecules are increasing in size due to coupling with nitrogen-containing molecules or hydrocarbons from food waste, thereby decreasing the O/C ratio and increasing the molecular mass. The way in which the trend holds true for both oxygen and nitrogen classes with near-equal periodicity indicates the phenomenon is a direct result of nitrogen-oxygen coupling reactions, such as the Maillard reaction. The maximum molecular mass of approximately 600 Da is due to limitations of the FT-ICR MS analysis technique and may also be indicative of capping reactions due to Maillard reactions.[25, 46, 47]

Discussion

Emergent Chemical Pathway Analysis

Figure 8 is a schematic representation of the reaction chemistry observed here under hydrothermal conditions, highlighting the emergent chemistries that only emerge upon blending feeds. Collectively, biocrude yields reported in **Figure 1** are consistent with the commonly held model that HTL involves hydrolysis and depolymerization of macromolecules that form short chain reactive species that then condense to form increasingly larger molecules that partition into the aqueous, organic, and solid phases, respectively.[2] Food and green waste feedstocks produce biocrude molecules with different levels of complexity and heteroatoms that promote specific chemical pathways when feedstocks are mixed in varying ratios prior to HTL. With food waste-rich blends, esterification reactions of the fatty acids and other oxygenates result in biocrude containing esters and an overall increase in the oxygen content of the biocrude relative to that obtained from pure food waste.[3] At equal HFW-GW blending ratios, which possess near-stoichiometric amounts of protein and carbohydrates, sharp decreases in oxygen classes and increased abundance in nitrogen-oxygen heteroatom classes are observed, consistent with reactions such as the Maillard reaction to couple reducing sugars and amino acid derivatives.[25] The 25:75 food waste:green waste blend undergoes more decarboxylation than the other feeds, resulting in a biocrude with relatively increased carbon number and DBE, indicative of polymerization reactions involving nitrogen reacting with cellulose and hemicellulose from green waste. Interestingly, the polymerization reactions terminate while molecules remain in the fuel-

range of the biocrude resulting from food waste, rather than forming heavy compounds in the residue range (**Figure 2**) or char phase (**Figure 1**)—both of which are otherwise prevalent in the products of different feeds, especially for HTL of food waste. While the green waste streams benefit from decarboxylation reactions that lower the oxygen heteroatomic content of the biocrude (**Figure 5**), the resulting mixture is more prone to char formation, resulting in insufficient capping to prevent polymerization.[48]

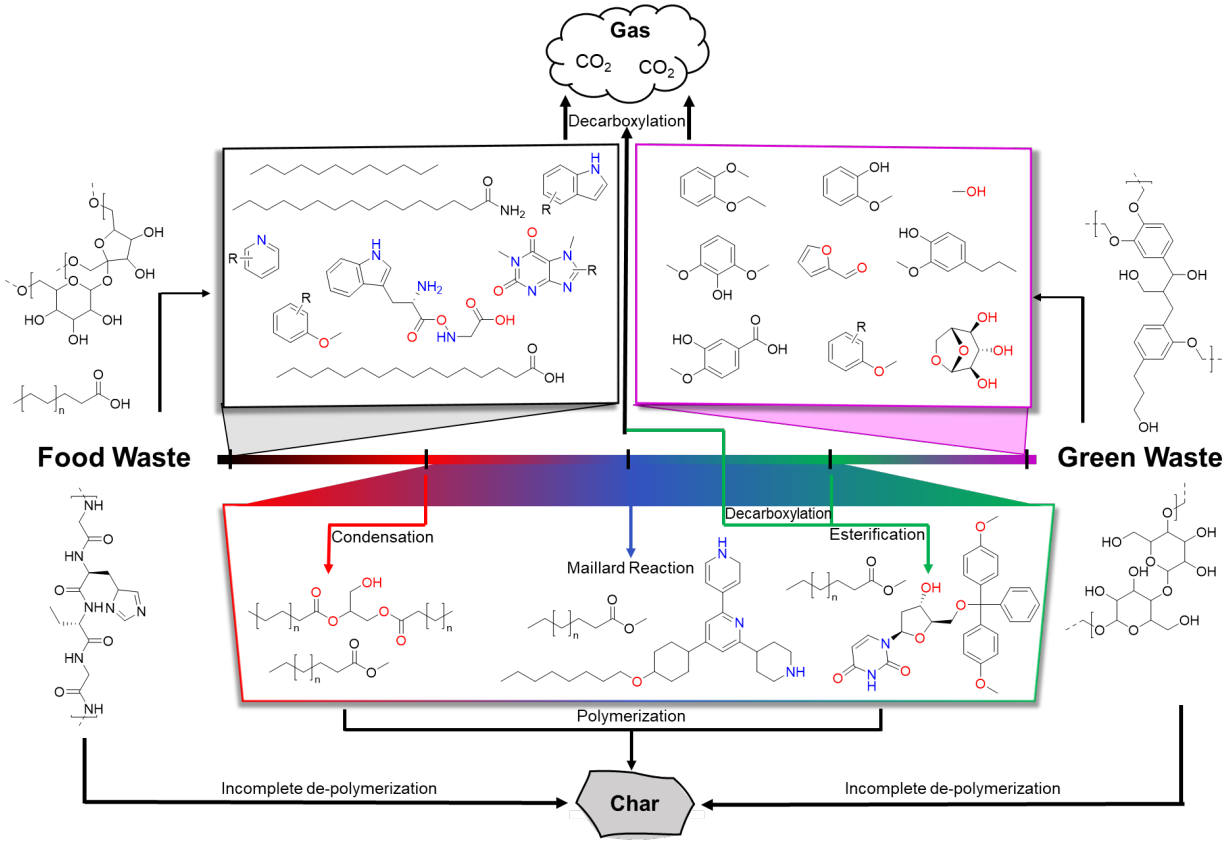

Figure 8. Chemical representation of characteristic molecules found in the biocrudes of the interactions between food and green waste components to produce new biocrude molecules.

The combined analytical observations provide a detailed picture of the chemical interactions that form biocrude from mixed food waste and green waste feedstocks. **Figure 8** captures the key molecular details governing HTL of pure food waste and green waste feedstocks as well as the transition to feed mixtures. Hydrolysis and thermolysis of proteins, lipids, and carbohydrates is represented by singular arrows from the feedstocks to the reactive intermediates.[49] Consistent with prior literature, food waste HTL results in a suite of fatty acids and nitrogen-containing compounds derived from food waste's protein content as well as the Maillard reaction

for the interaction between amino acid and sugar derivatives.[5, 32] Fatty acids and amides are confirmed primarily through the use of GC-MS, and the presence of substituted fatty amides is corroborated by the FT-ICR MS abundance at high H/C and low N/C values in **Figure 7**. The formation of char can progress through hydrothermal carbonization, whereby incomplete feedstock depolymerization is combined with repolymerization reactions to form insoluble products.[6] Additionally, polymerization of small molecules can continue until molecules are too large to remain soluble, thereby forming char.[50]

Emergent Chemistry

Emergent behavior arises from several sources, the simplest of which is transesterification of triglycerides from the lipid fraction of food waste and the esterification of their fatty acid derivatives. **Figure 8** shows the composition-dependent interactions giving rise to increased biocrude yield in a 75% food waste, 25% green waste feedstock mixture arising from coupling reactions with cellulose and lignin monomers and also resulting in higher-than-expected oxygen content in that biocrude (**Figure SI-5**). HTL of food waste-rich feeds is associated with high biocrude yields, and the chemical composition of the corresponding biocrudes contain substantial fractions of fatty acids and fatty amides that were not fully converted to aliphatic FAMEs.[3, 51] By introducing green waste, the transesterification drastically reduces the fatty acid content, favoring production of FAMEs, as observed by the GC-MS peak areas for fatty acids and FAMEs in the mixed-feed biocrudes, particularly the 25:75 mixture shown in **Figure 4b**. Notably, FAMEs are not identified in either of the pure food or green waste biocrudes due to the lack of methanol, resulting in solely hydrolysis. Due to their high abundance in the 25:75 biocrude, it can be interpreted that FAME production in mixed-feed HTL requires high concentrations of cellulose, lignin, or ash. As the carbohydrate content of both food and green waste primarily decompose to glucose and its derivatives,[52] the FAME production is most likely enabled by reaction with lignin derivatives. Lignin has been shown to produce methanol upon decomposition at elevated temperatures,[53] which allows for the transesterification reaction for FAME synthesis.[54] The transesterification reaction is a well-studied reaction pathway for the synthesis of fatty acid methyl esters for biodiesel from the reaction of fatty acids with methanol.[54]

Coupling reactions primarily impact compounds present in the diesel boiling point range, increasing them to a higher percentage than pure green waste biocrude and causing a corresponding

decrease in the jet fuel range, meaning that emergent chemistry will not be captured in volatility-based gas chromatography. The esterification of fatty acids supports the increased fraction of diesel-range compounds in the 75:25 biocrude from thermogravimetric analysis. FT-IR highlights the presence of strong C-O stretching bands indicative of cellulose and lignin-based molecules, as expected, whereas FT-ICR MS identifies the greatest number of molecular formulae without nitrogen, a key factor in increased biocrude quality and upgrading potential.

In addition to FAME production, further evidence of emergent behavior is found in polymerization Maillard-type reactions that react amino acids from the food waste proteins and oxygenates from the lignocellulosic green waste carbohydrates. **Figure 5** shows increased $N_{1\text{-}2}O_{1\text{-}4}$ molecular abundance in the 50:50 biocrude compared to the expected value, coupled with a near-equal decrease in pure oxygenated heteroatom class abundance. This trend is consistent with Maillard-type reactions observed previously in hydrothermal food waste mixtures.[25, 30, 55] Maillard reactions occur between reducing sugars from cellulose decomposition with the food waste decomposition product of amino acids and is most prevalent in stoichiometric ratios. **Figure 8** shows the composition-dependent reaction that gives rise to the equivalent N/C and O/C periodicity shown in **Figure 7**, consistent with increased relative abundance in the N_xO_y heteroatom classes in the 50:50 biocrude shown in **Figure 5**.

Decarboxylation of the heavily oxygenated biocrude formed from green waste and food waste is a final observation that can only be explained by emergent chemical pathways. Without this emergent chemistry, the pure feeds are prone to over-polymerization to chars, as observed with higher char yields (**Figure 1)** and heavy residue fractions in the pure feed biocrudes (**Figure 2**). When even a small fraction of food waste is blended into green waste, enhanced decarboxylation occurs, resulting in increased gas and char yields in the 25:75 reactions. Decarboxylation is a step in polymerization, removing CO_2 to combine molecules together in the same way that hydrolysis reactions enhance polymerization.[56, 57] Decarboxylation also plays a role in the decreased O_x class abundance seen with FT-ICR MS, and the increased nitrogen abundance from CHON. Borrowing from the hydrothermal carbonization (HTC) literature, lignocellulosic biomass has been shown to undergo extensive decarboxylation to char with increasing reaction severity (i.e. time and temperature), i.e., conditions that are milder yet similar to those used in this study.[58] Dissolved solids from cellulose and hemicellulose degradation polymerize in water via a

decarboxylative polymerization to form water insoluble polymers, as evidenced by the increased char fraction of the 25:75 blend, and heavy residue in the respective biocrude, as evidenced by the large residue fraction identified with TGA (**Figure 2**).[58, 59]

Co-liquefaction Benefits

Co-liquefaction introduces another layer of complexity to a reactive environment that already produces tens of thousands of unique compounds across three phases through thousands of reaction pathways. The present work shows that feeds can be strategically combined to suppress undesired chemistries present in the pure feedstocks while promoting desirable and new pathways, for example decarboxylation to minimize char formation or Maillard reactions to promote biocrude yields. While adding food waste to green waste does increase the nitrogen of the resulting biocrude, which will complicate subsequent upgrading efforts,[15, 60] thermogravimetric analysis and FT-ICR MS show that those nitrogen compounds cap the green waste biocrudes to usable molecular weights that would otherwise contain the highest fraction of residue-range compounds, typically regarded as un-usable. Accordingly, adding green waste to food waste does not drastically detract from biocrude quality and has the potential to increase yields while further buffering the supply chain with the addition of plentiful lignocellulosic waste. Co-processing also results in increased energy recovery compared with otherwise low-yielding lignocellulosic wastes, a frequent problem, while also increasing quality by partially deoxygenating prior to downstream refining. Further research should explore the effect of green waste composition on yields and biocrude quality.

Conclusion

Co-processing of a green waste and food waste stream was studied under HTL conditions, with subsequent molecular analysis of the biocrude products. Co-processing of a high-lipid food waste with up to 25% cellulose-rich lignocellulosic green waste results in biocrude yields greater than 45% and energy recovery greater than 50%. HTL of blended food and green waste streams resulted in emergent chemical behavior that promotes oil yields at low blend ratios by a combination of esterification, Maillard reactions, and polymerizations. GC-MS revealed the emergence of fatty acid methyl esters in mixed-feed HTL biocrudes that were not present in either individual feedstock. Thermogravimetric analysis confirmed desired molecule size and volatility emergence in the biocrudes before molecular level analysis was performed using (+) APPI FT-ICR MS to reveal deoxygenation and capping trends.

This work begins to unravel the complex reaction networks associated with hydrothermal waste conversion, illuminating both mechanisms and strategies for controlling product distributions, yields and quality using molecular-level feedstock engineering. Chemistries governing mixed-feed HTL were identified by examining heteroatom trends in biocrude products. An abundance of lignocellulosic material leads to over-polymerization via decarboxylation pathways due to high [OH] functionality pushing molecules from oil-soluble to the solid phase, whereas equal amounts of food and lignocellulosic-based molecules favor Maillard-type reactions that effectively terminate the polymerization at chain lengths that partition into the oil phases. Furthermore, these synergistic reactions result in CO_2 evolution, resulting in substantial deoxygenation and char mitigation. These findings greatly advance the scientific understanding of co-HTL as a practical strategy for biocrude maximization that can also improve supply chain management.

Acknowledgements

HOL was partially funded for this work by the National Science Foundation GRF Program under award number 2038257. We also acknowledge the Department of Energy Bioenergy Technology Office (DE-EE0008513) for funding this work. JRP was partially funded for this work by the Advanced Manufacturing for Energy Systems (AMES) fellowship at the University of Connecticut, funded by US Department of Energy Advanced Manufacturing Office traineeship program (DE-EE0008302). A portion of this work was performed at the National High Magnetic Field Laboratory, which is supported by the National Science Foundation Cooperative Agreement (DMR-1644779) and the state of Florida. All of the FT-ICR MS data are publicly available via the Open Science Framework https://osf.io/d3r8m/ (DOI 10.17605/OSF.IO/D3R8M).

References

1. Schanes, K.; Dobernig, K.; Gözet, B., Food waste matters - A systematic review of household food waste practices and their policy implications. *Journal of Cleaner Production* **2018,** *182*, 978-991.

2. LeClerc, H. O.; Tompsett, G. A.; Paulsen, A. D.; McKenna, A. M.; Niles, S. F.; Reddy, C. M.; Nelson, R. K.; Cheng, F.; Teixeira, A. R.; Timko, M. T., Hydroxyapatite catalyzed hydrothermal liquefaction transforms food waste from an environmental liability to renewable fuel. *iScience* **2022**, 104916.

3. Gollakota, A. R. K.; Kishore, N.; Gu, S., A review on hydrothermal liquefaction of biomass. *Renewable and Sustainable Energy Reviews* **2018,** *81*, 1378-1392.

4. Aierzhati, A.; Stablein, M. J.; Wu, N. E.; Kuo, C.-T.; Si, B.; Kang, X.; Zhang, Y., Experimental and model enhancement of food waste hydrothermal liquefaction with combined effects of biochemical composition and reaction conditions. *Bioresource Technology* **2019,** *284*, 139-147.

5. D.J. Zastrow, P. A. J. In *Hydrothermal Liquefaction of Food Waste and Model Food Waste Compounds*, AIChE, San Francisco, CA, San Francisco, CA, 2013.

6. Katakojwala, R.; Kopperi, H.; Kumar, S.; Venkata Mohan, S., Hydrothermal liquefaction of biogenic municipal solid waste under reduced H2 atmosphere in biorefinery format. *Bioresource Technology* **2020,** *310*, 123369.

7. Minowa, T.; Murakami, M.; Dote, Y.; Ogi, T.; Yokoyama, S.-y., Oil production from garbage by thermochemical liquefaction. *Biomass and Bioenergy* **1995,** *8* (2), 117-120.

8. Elliott, D. C.; Biller, P.; Ross, A. B.; Schmidt, A. J.; Jones, S. B., Hydrothermal liquefaction of biomass: Developments from batch to continuous process. *Bioresource Technology* **2015,** *178*, 147-156.

9. Mishra, R. K.; kumar, V.; Kumar, P.; Mohanty, K., Hydrothermal liquefaction of biomass for bio-crude production: A review on feedstocks, chemical compositions, operating parameters, reaction kinetics, techno-economic study, and life cycle assessment. *Fuel* **2022,** *316*, 123377.

10. Xu, Y.-H.; Li, M.-F., Hydrothermal liquefaction of lignocellulose for value-added products: Mechanism, parameter and production application. *Bioresource Technology* **2021,** *342*, 126035.

11. Cheng, F.; Belden, E. R.; Li, W.; Shahabuddin, M.; Paffenroth, R. C.; Timko, M. T., Accuracy of predictions made by machine learned models for biocrude yields obtained from hydrothermal liquefaction of organic wastes. *Chemical Engineering Journal* **2022,** *442*, 136013.

12. Cheng, F.; Cui, Z.; Chen, L.; Jarvis, J.; Paz, N.; Schaub, T.; Nirmalakhandan, N.; Brewer, C. E., Hydrothermal liquefaction of high- and low-lipid algae: Bio-crude oil chemistry. *Applied Energy* **2017,** *206*, 278-292.

13. Bayat, H.; Dehghanizadeh, M.; Jarvis, J. M.; Brewer, C. E.; Jena, U., Hydrothermal Liquefaction of Food Waste: Effect of Process Parameters on Product Yields and Chemistry. *Frontiers in Sustainable Food Systems* **2021,** *5*.

14. Chen, W.-T.; Haque, M. A.; Lu, T.; Aierzhati, A.; Reimonn, G., A perspective on hydrothermal processing of sewage sludge. *Current Opinion in Environmental Science & Health* **2020,** *14*, 63-73.

15. Leng, L.; Zhang, W.; Peng, H.; Li, H.; Jiang, S.; Huang, H., Nitrogen in bio-oil produced from hydrothermal liquefaction of biomass: A review. *Chemical Engineering Journal* **2020,** *401*, 126030.

16. Li, H.; Liu, Z.; Zhang, Y.; Li, B.; Lu, H.; Duan, N.; Liu, M.; Zhu, Z.; Si, B., Conversion efficiency and oil quality of low-lipid high-protein and high-lipid low-protein microalgae via hydrothermal liquefaction. *Bioresource Technology* **2014,** *154*, 322-329.

17. Li, S.; Jiang, Y.; Snowden-Swan, L. J.; Askander, J. A.; Schmidt, A. J.; Billing, J. M., Techno-economic uncertainty analysis of wet waste-to-biocrude via hydrothermal liquefaction. *Applied Energy* **2021,** *283*, 116340.

18. Badgett, A.; Newes, E.; Milbrandt, A., Economic analysis of wet waste-to-energy resources in the United States. *Energy* **2019,** *176*, 224-234.

19. Jiang, Y.; Jones, S. B.; Zhu, Y.; Snowden-Swan, L.; Schmidt, A. J.; Billing, J. M.; Anderson, D., Techno-economic uncertainty quantification of algal-derived biocrude via hydrothermal liquefaction. *Algal Research* **2019,** *39*, 101450.

20. LJ Snowden-Swan, Y. Z., SB Jones, DC Elliot, AJ Schmidt, RT Hallen, JM Billing, TR Hart, SP Fox, GD Maupin, Hydrothermal Liquefaction and Upgrading of Municipal Wastewater Treatment Plant Sludge: A Preliminary Techno-Economic Analysis. Energy, D. o., Ed. 2016.

21. Agency, U. S. E. P., National Overview: Facts and Figures on Materials, Wastes and Recycling. epa.gov, 2021.

22. Yang, L.; He, Q.; Havard, P.; Corscadden, K.; Xu, C.; Wang, X., Co-liquefaction of spent coffee grounds and lignocellulosic feedstocks. *Bioresource Technology* **2017,** *237*, 108-121.

23. Jarvis, J. M.; Billing, J. M.; Corilo, Y. E.; Schmidt, A. J.; Hallen, R. T.; Schaub, T. M., FT-ICR MS analysis of blended pine-microalgae feedstock HTL biocrudes. *Fuel* **2018,** *216*, 341-348.

24. Yang, J.; He, Q.; Yang, L., A review on hydrothermal co-liquefaction of biomass. *Applied Energy* **2019,** *250*, 926-945.

25. LeClerc, H. O.; Atwi, R.; Niles, S. F.; McKenna, A.; Timko, M. T.; West, R. H.; Teixeira, A. R., Elucidating the role of reactive nitrogen intermediates in hetero-cyclization during hydrothermal liquefaction of food waste. *Green Chemistry* **2022**.

26. Adewuyi, A., Underutilized Lignocellulosic Waste as Sources of Feedstock for Biofuel Production in Developing Countries. *Frontiers in Energy Research* **2022,** *10*.

27. Agency, E. P., RIN Trades and Price Information. 2021; Vol. 2021.

28. Debra L. Kantner, B. F. S. *Analysis of MSW Landfill Tipping Fees*; Environmental Research & Education Foundation: April 2019, 2019.

29. Biller, P.; Sharma, B. K.; Kunwar, B.; Ross, A. B., Hydroprocessing of bio-crude from continuous hydrothermal liquefaction of microalgae. *Fuel* **2015,** *159*, 197-205.

30. Déniel, M.; Haarlemmer, G.; Roubaud, A.; Weiss-Hortala, E.; Fages, J., Hydrothermal liquefaction of blackcurrant pomace and model molecules: understanding of reaction mechanisms. *Sustainable Energy & Fuels* **2017,** *1* (3), 555-582.

31. Cheng, F.; Tompsett, G. A.; Fraga Alvarez, D. V.; Romo, C. I.; McKenna, A. M.; Niles, S. F.; Nelson, R. K.; Reddy, C. M.; Granados-Fócil, S.; Paulsen, A. D.; Zhang, R.; Timko, M. T., Metal oxide supported Ni-impregnated bifunctional catalysts for controlling char formation and maximizing energy recovery during catalytic hydrothermal liquefaction of food waste. *Sustainable Energy & Fuels* **2021,** *5* (4), 941-955.

32. Cheng, F.; Tompsett, G. A.; Murphy, C. M.; Maag, A. R.; Carabillo, N.; Bailey, M.; Hemingway, J. J.; Romo, C. I.; Paulsen, A. D.; Yelvington, P. E.; Timko, M. T., Synergistic Effects of Inexpensive Mixed Metal Oxides for Catalytic Hydrothermal Liquefaction of Food Wastes. *ACS Sustainable Chemistry & Engineering* **2020,** *8* (17), 6877-6886.

33. Maag, A. R.; Paulsen, A. D.; Amundsen, T. J.; Yelvington, P. E.; Tompsett, G. A.; Timko, M. T., Catalytic Hydrothermal Liquefaction of Food Waste Using CeZrOx. *Energies* **2018,** *11* (3).

34. Stein, S. E., Estimating probabilities of correct identification from results of mass spectral library searches. *Journal of the American Society for Mass Spectrometry* **1994,** *5* (4), 316-323.

35. Chen, J.; Li, S., Characterization of biofuel production from hydrothermal treatment of hyperaccumulator waste (Pteris vittata L.) in sub- and supercritical water. *RSC Advances* **2020,** *10* (4), 2160-2169.

36. Stankovikj, F.; McDonald, A. G.; Helms, G. L.; Garcia-Perez, M., Quantification of Bio-Oil Functional Groups and Evidences of the Presence of Pyrolytic Humins. *Energy & Fuels* **2016,** *30* (8), 6505-6524.

37. Hendrickson, C. L.; Quinn Jp Fau - Kaiser, N. K.; Kaiser Nk Fau - Smith, D. F.; Smith Df Fau - Blakney, G. T.; Blakney Gt Fau - Chen, T.; Chen T Fau - Marshall, A. G.; Marshall Ag Fau - Weisbrod, C. R.; Weisbrod Cr Fau - Beu, S. C.; Beu, S. C., 21 Tesla Fourier Transform Ion Cyclotron Resonance Mass Spectrometer: A National Resource for Ultrahigh Resolution Mass Analysis. **2015,** (1879-1123 (Electronic)).

38. Smith, D. F.; Podgorski, D. C.; Rodgers, R. P.; Blakney, G. T.; Hendrickson, C. L., 21 Tesla FT-ICR Mass Spectrometer for Ultrahigh-Resolution Analysis of Complex Organic Mixtures. *Analytical Chemistry* **2018,** *90* (3), 2041-2047.

39. Zhang, B.; Zhong, Z.; Min, M.; Ding, K.; Xie, Q.; Ruan, R., Catalytic fast co-pyrolysis of biomass and food waste to produce aromatics: Analytical Py–GC/MS study. *Bioresource Technology* **2015,** *189*, 30-35.

40. Zhang, H.; Cheng, Y.-T.; Vispute, T. P.; Xiao, R.; Huber, G. W., Catalytic conversion of biomass-derived feedstocks into olefins and aromatics with ZSM-5: the hydrogen to carbon effective ratio. *Energy & Environmental Science* **2011,** *4* (6), 2297-2307.

41. Haider, M. S.; Castello, D.; Michalski, K. M.; Pedersen, T. H.; Rosendahl, L. A., Catalytic Hydrotreatment of Microalgae Biocrude from Continuous Hydrothermal Liquefaction: Heteroatom Removal and Their Distribution in Distillation Cuts. *Energies* **2018,** *11* (12).

42. Tan, K. T.; Lee, K. T.; Mohamed, A. R., Production of FAME by palm oil transesterification via supercritical methanol technology. *Biomass and Bioenergy* **2009,** *33* (8), 1096-1099.

43. O'Sullivan, A. C., Cellulose: the structure slowly unravels. *Cellulose* **1997,** *4* (3), 173-207.

44. Ralph, J.; Lapierre, C.; Boerjan, W., Lignin structure and its engineering. *Current Opinion in Biotechnology* **2019,** *56*, 240-249.

45. Rodgers, R. P.; McKenna, A. M., Petroleum Analysis. *Analytical Chemistry* **2011,** *83* (12), 4665-4687.

46. LeClerc, H. O.; Atwi, R.; Niles, S. F.; McKenna, A. M.; Timko, M. T.; West, R. H.; Teixeira, A. R., Elucidating the role of reactive nitrogen intermediates in hetero-cyclization during hydrothermal liquefaction of food waste. *Green Chemistry* **2022**.

47. McKenna, A. M.; Nelson, R. K.; Reddy, C. M.; Savory, J. J.; Kaiser, N. K.; Fitzsimmons, J. E.; Marshall, A. G.; Rodgers, R. P., Expansion of the Analytical Window for Oil Spill Characterization by Ultrahigh Resolution Mass Spectrometry: Beyond Gas Chromatography. *Environmental Science & Technology* **2013,** *47* (13), 7530-7539.

48. Tao, W.; Yang, X.; Li, Y.; Zhu, R.; Si, X.; Pan, B.; Xing, B., Components and Persistent Free Radicals in the Volatiles during Pyrolysis of Lignocellulose Biomass. *Environmental Science & Technology* **2020,** *54* (20), 13274-13281.

49. Motavaf, B.; Savage, P. E., Effect of Process Variables on Food Waste Valorization via Hydrothermal Liquefaction. *ACS ES&T Engineering* **2021,** *1* (3), 363-374.

50. Cantero-Tubilla, B.; Cantero, D. A.; Martinez, C. M.; Tester, J. W.; Walker, L. P.; Posmanik, R., Characterization of the solid products from hydrothermal liquefaction of waste feedstocks from food and agricultural industries. *The Journal of Supercritical Fluids* **2018,** *133*, 665-673.

51. Gärtner, C. A.; Serrano-Ruiz, J. C.; Braden, D. J.; Dumesic, J. A., Catalytic Upgrading of Bio-Oils by Ketonization. *ChemSusChem* **2009,** *2* (12), 1121-1124.

52. Shen, D. K.; Gu, S., The mechanism for thermal decomposition of cellulose and its main products. *Bioresource Technology* **2009,** *100* (24), 6496-6504.

53. Ander, P.; Eriksson, K.-E., Methanol formation during lignin degradation by Phanerochaete chrysosporium. *Applied Microbiology and Biotechnology* **1985,** *21* (1), 96-102.

54. Gerpen, J. V., Biodiesel processing and production. *Fuel Processing Technology* **2005,** *86* (10), 1097-1107.

55. Chen, Y.; Wu, Y.; Ding, R.; Zhang, P.; Liu, J.; Yang, M.; Zhang, P., Catalytic hydrothermal liquefaction of D. tertiolecta for the production of bio-oil over different acid/base catalysts. *AIChE Journal* **2015,** *61* (4), 1118-1128.

56. Gao, H.-Y.; Held, P. A.; Knor, M.; Mück-Lichtenfeld, C.; Neugebauer, J.; Studer, A.; Fuchs, H., Decarboxylative Polymerization of 2,6-Naphthalenedicarboxylic Acid at Surfaces. *Journal of the American Chemical Society* **2014,** *136* (27), 9658-9663.

57. Zhou, H.; Zhang, F.; Wang, R.; Lai, W.-M.; Xie, S.; Ren, W.-M.; Lu, X.-B., Facile Access to Functionalized Poly(thioether)s via Anionic Ring-Opening Decarboxylative Polymerization of COS-Sourced α-Alkylidene Cyclic Thiocarbonates. *Macromolecules* **2021,** *54* (22), 10395-10404.

58. Guo, S.; Dong, X.; Liu, K.; Yu, H.; Zhu, C., Chemical, Energetic, and Structural Characteristics of Hydrothermal Carbonization Solid Products for Lawn Grass. *2015* **2015,** *10* (3), 13.

59. Funke, A.; Ziegler, F., Hydrothermal carbonization of biomass: A summary and discussion of chemical mechanisms for process engineering. *Biofuels, Bioproducts and Biorefining* **2010,** *4* (2), 160-177.

60. Obeid, F.; Chu Van, T.; Brown, R.; Rainey, T., Nitrogen and sulphur in algal biocrude: A review of the HTL process, upgrading, engine performance and emissions. *Energy Conversion and Management* **2019,** *181*, 105-119.